

INTENSIVE RESOLUTION MEASUREMENT WITH THE SAMDIS MULTI-ASPECT SYNTHETIC APERTURE SONAR

Nicolas BURLET	Thales DMS France SAS
Yann LE GALL	Thales DMS France SAS
Sebastien DELAYES	Thales DMS France SAS
Samantha DUGELAY	Thales UK
Fabien NOVELLA	DGA TN

Contact : Nicolas.Burlet@fr.thalesgroup.com

1 INTRODUCTION

In the field of mine warfare, improving synthetic aperture sonar (SAS) resolution in order to detect and classify increasingly complex threats is of great interest. Resolution is clearly a fundamental and objective parameter of a sonar (even if the method to measure this resolution is sometimes subject to debate).

The quality of a SAS image is affected by multiple factors, such as ambient noise, vehicle instability, propagation conditions, physical and acoustic environment, multiple path, processing, etc. Thus, it seems relatively intuitive to recognize a "bad" image: high side lobes, saturation, defocusing, low contrast, etc. Several interesting illustrations can be found in the article from R.E Hansen ¹. Other illustrations are visible on Figure 1.

As already pointed by J. Dillon², beautiful sonar images are often presented by sonar manufacturers and especially on wrecks (ships, planes, etc.). Figure 2 is really nice. However, for a mine warfare application, the sonar response of a small object (typically 1mx1m) is more interesting for the end user. Moreover, usually we don't know how the image was obtained. With a real-time embedded processing or after hours of hand-tuned post-processing in a laboratory? Is this image statistically representative of the other images acquired by the sonar? Does it really qualify the sonar performances?

AL van Velsen³ explains that "Relevant performance criteria depend on the application for which the system is to be used". In other words and more complete, a "good" sonar is a sonar that produces images with controlled reproducibility that allows the end user to efficiently perform the task it must accomplish using that image. And this is quite difficult to demonstrate.

In this article, we will recall some considerations on the along-track resolution measurement. We will then present the qualification method applied to the high-resolution multi-aspect Synthetic Aperture Mine Detection and Imaging Sonar (SAMDIS), and finally some statistically representative results that guarantee good performance for the end user.

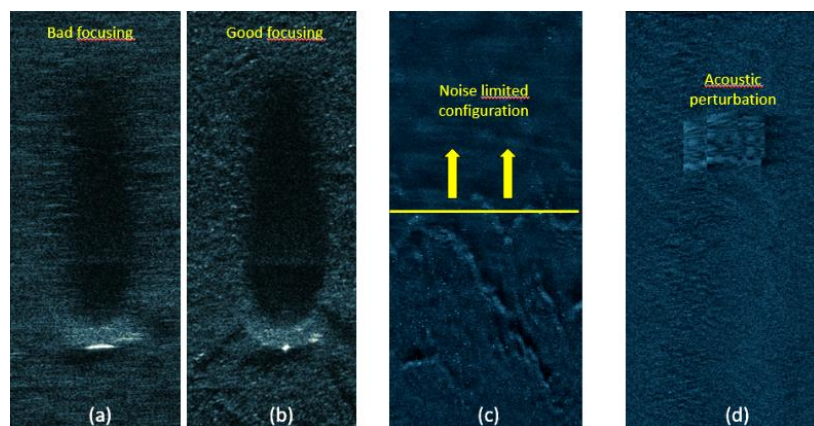


Figure 1 : Effect of focusing on images (a) and (b). Noise limited configuration on upper part of image (c). Acoustic perturbation on image (c)

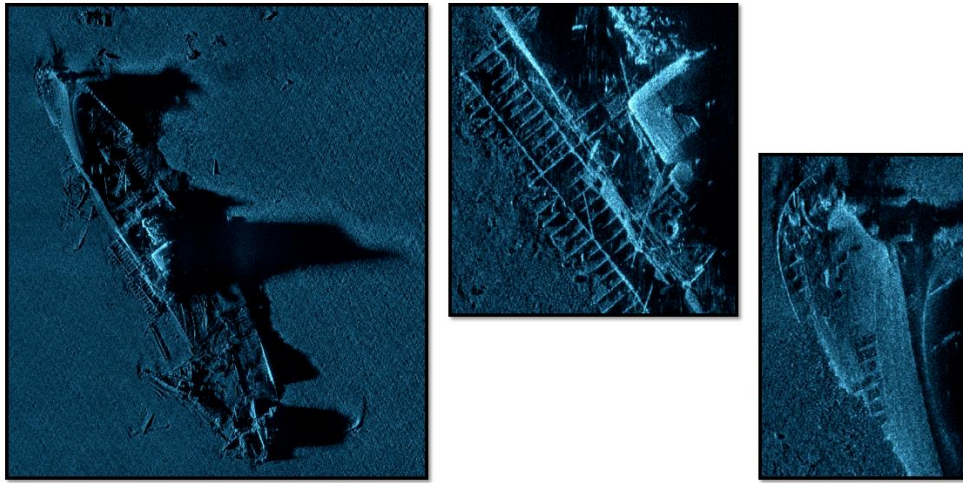


Figure 2 : SAMDIS SAS image from Thales – Swansea-Vale wreck

2 ALONG-TRACK RESOLUTION MEASUREMENT

2.1 Resolution measurement

The most used metric is probably resolution^{2,3,5,7}. Resolution⁹ is the ability to separate points of an object that are located at a small (angular) distance. It is important to remember this basic but physical definition because for a mine warfare operator, this is the ability to discriminate some small elements on a mine that may be the only differences with a natural rock, as can be seen on example¹⁰ below (red circles).

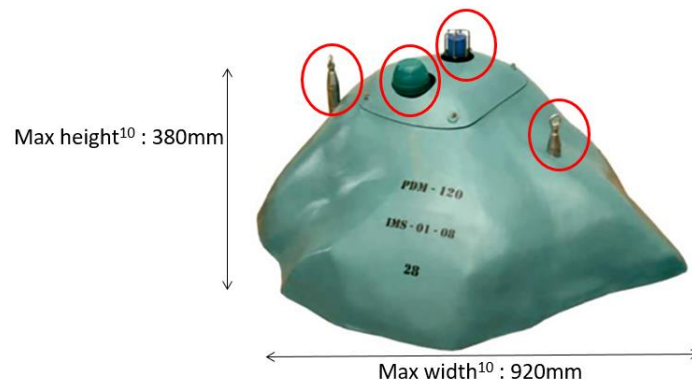


Figure 3 : PDM 120¹⁰ mine - Small potentially discriminating elements

The resolution measurement simply consists in the width measurement of the main lobe of the azimuth response of a point target. This method, sometimes called HPBW⁴ (Half Power Beam Width), is the result of the Rayleigh formulation⁸ in 1879 for optics problems: two point sources are regarded as just resolved when the zero-order diffraction maximum of one diffraction pattern coincides with the first minimum of the other.

For the case of a linear array (physical or synthetic) of length L , unshaded, and a cardinal sine beampattern, the application of the Rayleigh criteria leads to an angular resolution definition $2\theta_{4dB}$ equal to the -4dB beamwidth. If λ is the wavelength, we have the following relation:

$$2\theta_{4dB} = \frac{\lambda}{L} \quad (1)$$

However, conventionally, the resolution is taken equal to the -3dB beamwidth $2\theta_{3dB}$ and the previous equation becomes:

$$2\theta_{3dB} = 0.886 \frac{\lambda}{L} \quad (2)$$

For the same sonar, depending on the resolution definition, resolution can vary by more than 10%. It is therefore important to always clearly specify the chosen convention.

However this measurement can prove to be very irrelevant if the sidelobes are particularly high. We note δ_{3dB} , the along-track resolution at the distance R, for a -3dB angular resolution criteria:

$$\delta_{3dB} = R \cdot 2\theta_{3dB} \quad (3)$$

On Figure 4, theoretical 3dB resolution is equal to 4,4cm. We understand easily that even if the echo on the right figure reaches the theoretical resolution, quality of the signal on the left is really better. Maybe the signal on the right is badly focused or the target is not really a point target. But this problem cannot be detected if the sidelobes level is not analyzed.

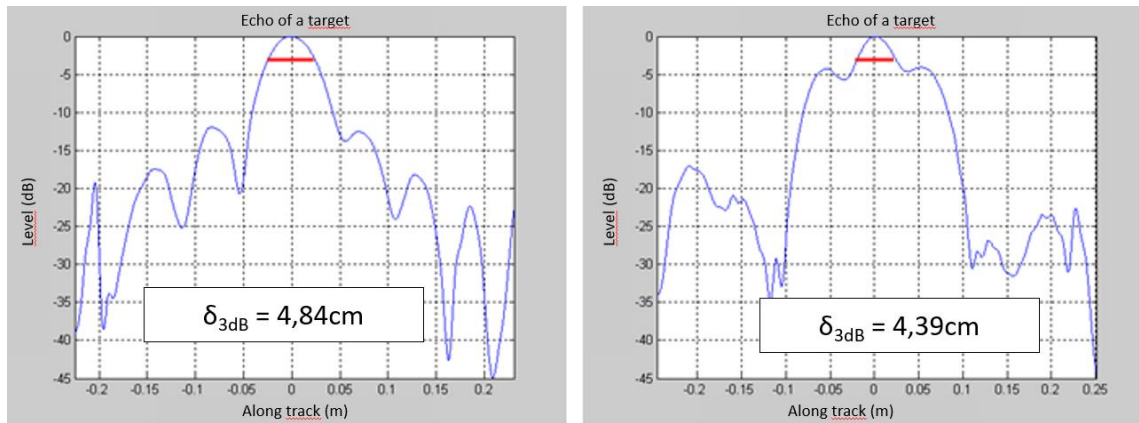


Figure 4 : 3dB resolution and sidelobes

So we recommend to measure the peak sidelobe ratio (PSLR⁴) which is the ratio between the peak intensity of the main lobe and the level of the first sidelobe. Other sidelobes could be interesting but depending on the target and the environment, they can quickly be disturbed. So, they are less reliable.

2.2 Statistical control of the along-track resolution

Unlike a conventional sonar, the resolution of a synthetic aperture sonar is not truly an intrinsic parameter of the system. This resolution has a stochastic nature as it is dependent on the environment.

Indeed, the along-track resolution of the SAS depends on the precision of self-calibration^{11,12,13}, which refers to the accuracy of estimating the array movements from ping to ping.

The gain of the synthetic aperture (and consequently the resolution) is then dependent on the cumulative phase errors along this aperture. If we consider that the bearing shift β estimated by P²C² (ping-to-ping cross-correlation) between two pings has a dominant effect on cumulated phase errors¹⁴, then the phase error $\sigma_{\Phi_{N,\beta}}$ along the synthetic aperture is expressed^{14,15} as:

$$\sigma_{\Phi_{N,\beta}} = \frac{4\pi VT_r}{\lambda} \sqrt{\frac{(N-1)^3}{3} - \frac{N-1}{12}} \sigma_{\beta} \quad (4)$$

Where σ_{β} is the standard deviation of β whose Cramer-Rao lower bound expression is well known¹², V is the sonar speed, λ the sonar wavelength, T_r the ping rate and N the number of integrated pings.

On the other hand, by Monte Carlo simulations, it is possible to calculate the probability that the degradation ΔQ of the gain of the synthetic array is less than a given value as a function of the cumulative phase error σ_{Φ_N} . The following curve¹¹ shows the probability $P(\Delta Q < 1dB)$ that the degradation ΔQ is less than 1dB.

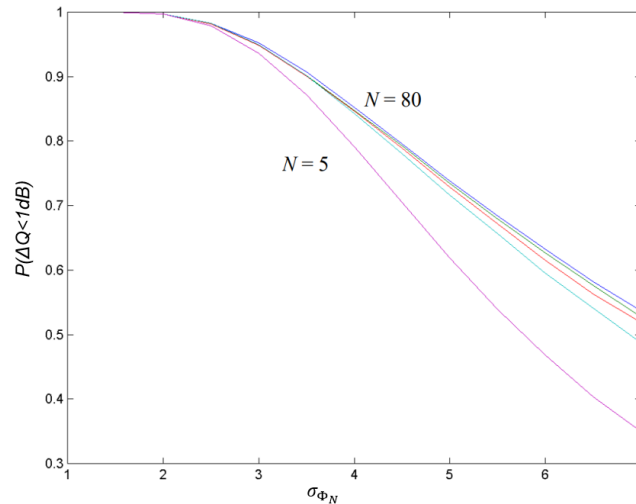


Figure 5 : probability that the degradation of the gain of the synthetic array is less than 1dB, function of the cumulative phase error and for different values of the number N of integrated pings

For example, we can choose¹¹ $\sigma_{\Phi_N} = 3,5$ to get the condition $P(\Delta Q < 1dB) = 90\%$. Therefore, combining this constraint and equation (5), while condition below is respected, we have a good statistical control of resolution.

$$\frac{4\pi VT_T}{\lambda} \sqrt{\frac{(N-1)^3}{3} - \frac{N-1}{12}} \sigma_\beta < 3,5 \quad (5)$$

This approach is interesting to better understand that specifying the resolution of a SAS is not enough and that it is preferable to associate it with the statistical framing of the degradation of this resolution. Similarly, the experimental verification of the resolution of a SAS cannot be limited to a few isolated measurements but must be sufficiently “intensive” to correctly take into consideration the stochastic nature of this resolution.

2.3 Methods and limits of along-track resolution measurement

2.3.1 Methods with specific target

Two kind of specific targets could be used to estimate the along-track resolution of a SAS: targets allowing to measure the 3dB beamwidth of the azimuth response of a point target and targets allowing to evaluate the physical resolvability of the sonar.

First case: 3dB beamwidth

In the first case, we generally use a target whose response is punctual, typically a sphere. This could be several “big” spheres (Figure 6) to have a high enough target strength, for example with a diameter between 50cm and 100cm. But sometimes, small spheres (diameter between 40mm and 80mm for example³) are used too.



Figure 6 : “Big” spheres used for resolution evaluation

It is quite simple to lay several “big” spheres on the sea bottom, to record different sonar tracks for several ranges and to carry out an intensive measurement campaign of the resolution. It is probably more difficult with small targets³ because of very low target strength. However, resolution measurements on this kind of target can be disturbed by rings or lifting hooks or even by algae or seashells present on the target.



Figure 7 : Algae or shells on spheres that can modify target response

Moreover, the assumption that the response of a sphere corresponds to a point target may turn out to be false for high SAS integration gains relative to the diameter of the sphere. Indeed, because of the migration of the specular echo on the circumference of the sphere, the closer one gets to the end of the synthetic antenna, the more the positions of the focusing point A and that of the specular echo B deviate (Figure 8).

On Figure 8, R is the distance between the center of the synthetic array and the focalization point A, r is the radius of the sphere, x is the along-track distance between the center of the synthetic array and the considered physical array, and R₁ the distance to the focalization point A. So, by focusing on point A, we commit a phase error linked to the fact that the position of the specular echo is actually at B.

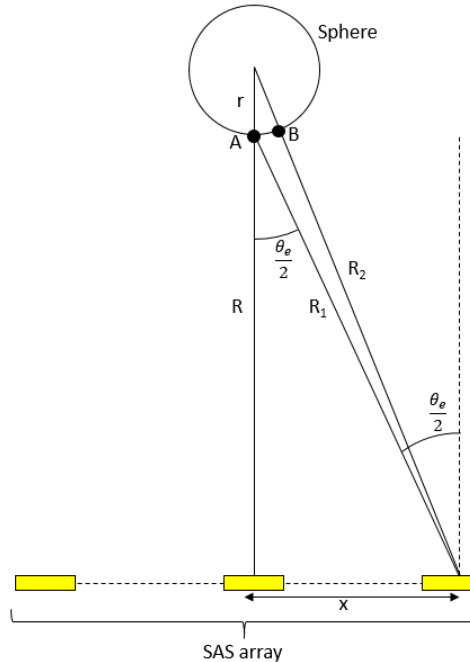


Figure 8 : SAS array and spherical target

This phase error δ_φ is then equal to:

$$\delta_\varphi = \frac{2\pi}{\lambda} 2(R_1 - R_2) = \frac{2\pi}{\lambda} 2 \left(R_1 - \left(\sqrt{(R+r)^2 + x^2} - r \right) \right) \text{ with } R_1 = \sqrt{R^2 + x^2} \quad (6)$$

So we have:

$$\delta_\varphi = \frac{4\pi}{\lambda} \left(R_1 - \left(\sqrt{(R^2 + x^2) \left(1 + \frac{r^2 + 2Rr}{R^2 + x^2} \right)} - r \right) \right) \quad (7)$$

With a first order Taylor expansion of the “square root” function and by considering that $r \ll R$, we get :

$$\delta_\varphi = \frac{4\pi}{\lambda} r \left(1 - \frac{R}{R_1} \right) \quad (8)$$

So, at the extremity of the SAS array, considering an integration all over the angle θ_e , we have the simple expression:

$$\delta_\varphi = \frac{4\pi}{\lambda} r \left(1 - \cos \frac{\theta_e}{2} \right) \quad (9)$$

A limit of the radius of the sphere could be established with the classical following constraint:

$$2r \left(1 - \cos \frac{\theta_e}{2} \right) < \frac{\lambda}{8} \quad (10)$$

Or equivalent :

$$r < \frac{\lambda}{16 \left(1 - \cos \frac{\theta_e}{2} \right)} \quad (11)$$

For example, Figure 9 shows the maximal sphere radius r function of integration angle θ_e for a sonar frequency of 300kHz. We can see that using spheres with a radius equal or greater than 0.5m is possible only if $\theta_e < 4^\circ$ (-3dB SAS resolution $> 3.2\text{cm}$)

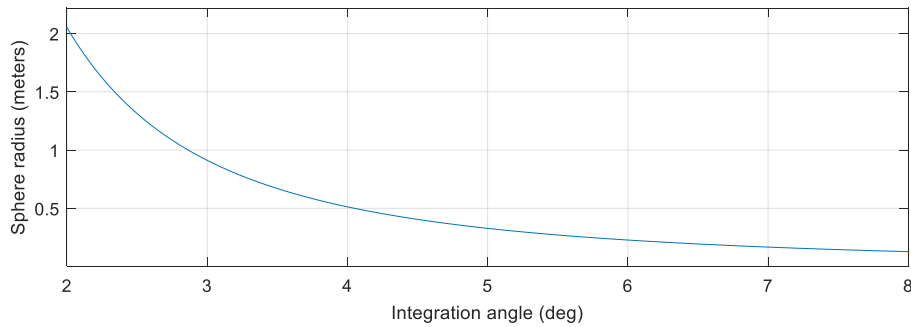


Figure 9 : Maximal sphere radius function of integration angle (freq=300kHz)

Second case: physical resolvability

In the second case, targets are sometimes designed and manufactured specially to evaluate the ability of the system to separate two very close targets, such as multiple parallel bars¹⁶ or small balls attached to a cross¹⁶.

This method is very interesting because it perfectly corresponds to the physical and operational definition of the resolution (capacity to discriminate two points). However, this kind of targets generally only allow a qualitative and visual evaluation of the resolution of the images because in case of defocusing, the targets being very close to each other, the signals tend to mix.

2.3.2 Methods without specific target

It is obviously very tempting to try to implement methods for measuring resolution without having to deploy specific targets at sea. These methods^{5,7} often rely on a statistical approach where the image is assumed to contain natural point-like objects. These methods seems to be interesting to give an indication of the image quality. However, they are not precise enough to really qualify the resolution of the sonar.

Other methods try to directly use the reverberation², but they are more detached from the physical meaning of resolution. And the comparison of the accuracy of the resolution measurement between such a method and the classical method based on the half power beam width still needs to be proven experimentally.

3 QUALIFICATION METHOD APPLIED FOR SAMDIS SONAR

The high resolution multi-aspect Synthetic Aperture Mine Detection and Imaging Sonar (SAMDIS) from Thales has already been the subject of publications^{15,17,18}. In this article, we will focus more particularly on the resolution of the following two modes:

- The SAS multi-aspect mode, able to deliver in real-time 3 SAS images of the area with 3 different views (-30° backward, broadside and 30° forward), with 5cm along track resolution
- The SAS high resolution mode, able to deliver in real-time a very high-resolution broadside SAS image with 2.5cm along track and 1.25 cm across-track,

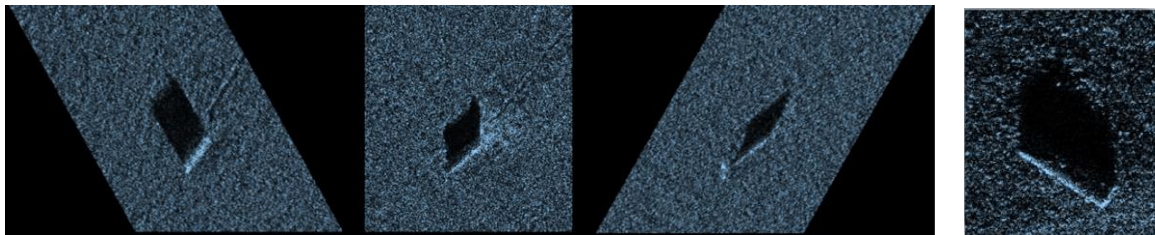


Figure 10 : SAS Multi-aspect images of a cylinder on the left, SAS high resolution image of a cylinder on the right

In 2015, sea trials have been performed in Douarnenez Bay and Brest Bay (France), in the scope of the French Espadon project. The SAMDIS sonar was mounted on an A27 Unmanned Underwater Vehicle (UUV) and several tracks were realized over targets on different bottoms:

- 4 different sea bottoms have been tested (from mud to rock)
- Water depth was typically between 20m and 30m
- Approximately one hundred targets were laid on the seabed, from “classical” objects (sphere, cylinder, truncated cone) to more stealthy targets
- The range of the targets was generally between 40m and 150m.
- The diameter of the spherical targets used for the resolution measurements was approximately between 50cm and 80cm.

About 140 resolution measurements were carried out for the SAS multi-aspect mode and 30 measurements for the SAS high resolution mode.

As shown in Figure 6, spherical targets were not perfect because of lifting hooks sometimes visible. However, this problem was overcome thanks to the large number of recordings made by varying the points of views on the targets (variation of the distance, of the azimuth, etc.).

For the SAS high resolution mode, the angular range of integration θ_e is equal to 5.7° approximately to provide an along-track resolution (at -3dB) of 2.22cm. Therefore, to respect the constraint of equation (11), the maximum radius of the spherical target should be limited to 25cm. This means that the spheres used for resolution measurements are slightly too big. The degradation of the synthetic beam pattern with a spherical radius equal to 40cm (worst case) can be predicted with a simple simulation and with equation (6).

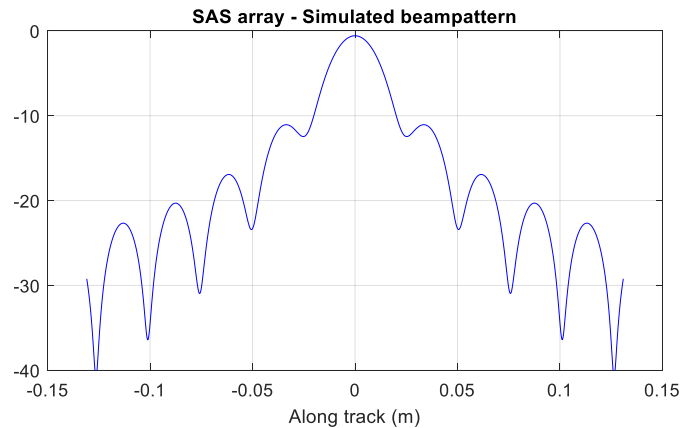


Figure 11 : SAS array – Simulated response of a spherical target with 40cm radius and for an along-track resolution at -3dB of 2.22cm

On Figure 11, we observe the impact of a spherical target with 40cm radius:

- 3dB beamwidth is equal to 2.31cm instead of 2.22cm
- Sidelobe level is degraded by 2.75dB
- Decrease of the gain of 0.58dB

Generally speaking, sonar performance is estimated using data acquired from the operational embedded and real-time mode, meaning that there is no modification of the processing or post-processing in a laboratory.

All measurements are performed on both sides of the sonar (port/starboard), for all three aspects (in multi-aspect mode), and at various ranges.

The resolution measurements are conducted on spherical targets by measuring the 3dB width of the specular echo (see §2.1). To achieve fine measurement, the oversampling factor of the synthetic beams is increased. This is the only modification compared to the operational processing.

The SAMDIS desired resolution is equal to 5cm for multi-aspect mode and 2.5cm for high resolution mode. But in order to ensure that at least 95% of the resolution measurements are better than the desired resolution, SAS algorithm is configured as follows: $\delta_{3dB} = 4.43\text{cm}$ (multi-aspect mode) and 2.22cm (high resolution).

4 RESULTS

This part presents all the measurements of along-track resolution function of the distance as well as the average level of the secondary lobes.

Multi-aspect resolution

In Figure 12, all the along-track resolution measurements (3 aspects) are shown together because there is no significant dependence of the results with the aspect. Figure 12a shows all the measurements with a target range from 40m to almost 180m. The mean value of the resolution is equal to 4.49cm, which is very close to the theoretical expected value (error of only 0.6mm). Moreover, we can consider that the mean value is independent on the range (dashed red tendency curve on Figure 12 left).

On Figure 12 (right), we can see that **96% of the resolution measurements are better than 5cm**.

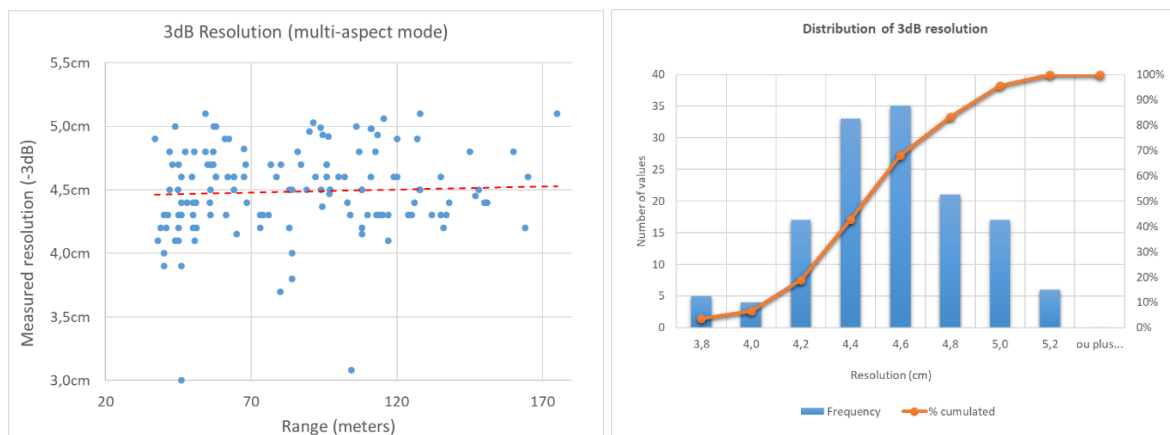


Figure 12 : SAS Multi-aspect resolution measurements (left) and distribution (right)

High-resolution mode

Figure 13 (left) shows the measurements with a target range from 35m to 145m. The mean value of the resolution is equal to 2.33cm, which is slightly higher than the theoretical value (2.22cm). The mean value is independent of range (dashed red curve on the figure).

On Figure 13 (right), we can see that 81% of the resolution measurements are better than 2.5cm and 94% are better than 2.6cm, which is really a good result.

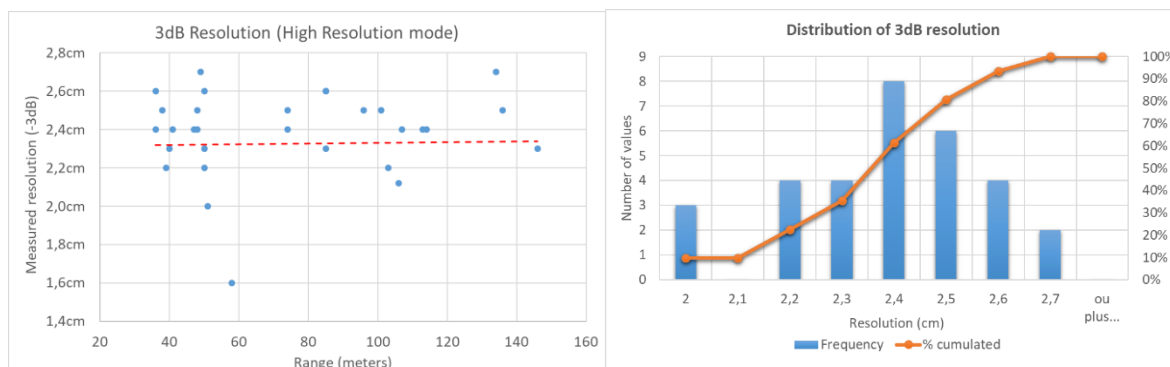


Figure 13 : High Resolution mode, resolution measurements (left) and distribution (right)

This very slight performance degradation (~1mm), compared to what we observed in the multi-aspect mode, could be due to the size of the spherical targets (Figure 11) and to small errors of the sound speed measured in situ. Sensitivity with sound speed is well known¹⁶. These kind of errors can be easily corrected in post-processing with an autofocus algorithm¹⁴.

Sidelobe level

If “Ev” denotes the theoretical expected value of the sidelobe level then the mean measured value of the sidelobe levels is equal to “Ev-0.7dB” (so the measured mean value is better than the expected one) and the standard deviation is equal to 4dB.

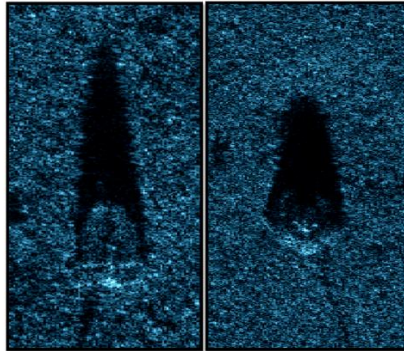


Figure 14 : High resolution mode images - a stealthy wedge (left), truncated cone (right)

5 CONCLUSION

The quality of SAMDIS sonar has been verified through rigorous statistical analysis, by performing measurements on physical targets, in a variety of environments and for all operational ranges. The resolution setting in SAS processing is oversized to ensure, not average resolution, but about 2 sigma resolution. Thus, **95% of the measurements are always better than the announced resolution.**

As mentioned in the introduction, a good sonar is a sonar that allows the end user to efficiently perform the task it must accomplish. And it is precisely this controlled quality of sonar performances in all circumstances (environment, range, shallow water, etc.) that allows us to guarantee the final operating quality, especially for detection and classification.

Results of this operational performance was presented very recently²¹. This evaluation was carried out on very challenging operational scenarios. Here are some key figures :

- 200 km² covered during day and night
- Depth from 7m to 300m
- Sea state 3, wind 25 knots (35 knots in gust), 3 knots of current
- Several thousand contacts
- Very dense areas (Figure 15)

Depending on the scenario, classification probabilities were between 95% and 99% and false alarm probabilities between 1% and 2%, which represents a real breakthrough in such demanding environments.

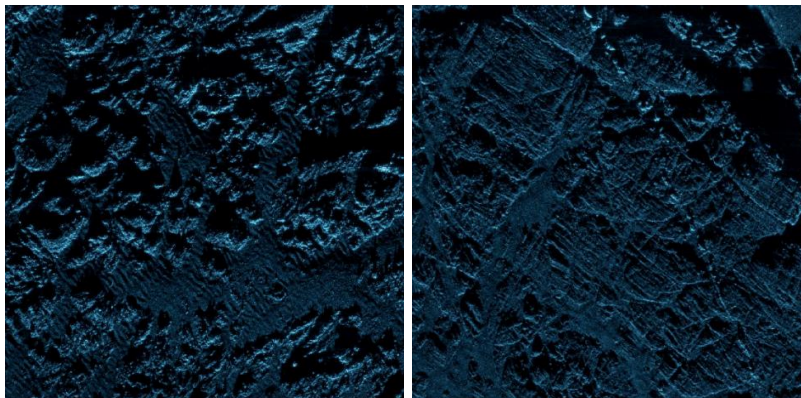


Figure 15 : Examples of challenging environments used for SAMDIS operational performance evaluation²¹

6 ACKNOWLEDGMENT

The authors wish to acknowledge DGA/UM-NAV, French Navy and DGA TN for their support and authorization to publish this paper.

7 REFERENCES

1. R.E Hansen, H.J Callow, T.O Sæbø, Challenges in Seafloor Imaging and Mapping With Synthetic Aperture Sonar, IEEE Transactions on Geoscience and Remote Sensing, Vol. 49, no. 10, (October 2011).
2. J. Dillon and R. Charron, Resolution Measurement for Synthetic Aperture Sonar, OCEANS 2019 MTS/IEEE, Seattle, WA, USA, pp. 1-6 , (2019)
3. AL van Velsen, Side looking sonar image quality assessment using reference targets, 4th International Conference on SAS and SAR (September 2018)
4. S. Kumar Das, Synthetic Aperture Radar Image Quality Measurements, thesis, Blekinge Institute of Technology (June, 2011)
5. N.P. Glover, I Campbell, Simultaneous Low and High frequency High Resolution SAS and a Statistical Method of Quantifying the Resolutions Obtained, Proceedings of the Institute of Acoustics Volume 32 Pt.4, Lerici, Italy (13-14 sept. 2010)
6. M. Couillard, J. Groen, W.L. Fox, Performance assessment of the MUSCLE synthetic aperture sonar, ECUA 2012
7. J. L. Prater, J. L. King and D. C. Brown, Determination of image resolution from SAS image statistics, OCEANS 2015 - MTS/IEEE Washington, USA (2015)
8. SL. Rayleigh, "Investigations in optics, with special reference to the spectroscope," Phil. Mag. 8, (1879).
9. https://en.wikipedia.org/wiki/Angular_resolution
10. <https://lilltech-defence.eu/underwater-bottom-mine-pdm-120/>
11. D. Billon and F. Fohanno, Two improved ping-to-ping cross-correlation methods for synthetic aperture sonar: theory and sea results," OCEANS '02 MTS/IEEE, Biloxi, MI, USA (2002)
12. D. Billon and F. Fohanno, Theoretical performance and experimental results for synthetic aperture sonar self-calibration, IEEE Oceanic Engineering Society. OCEANS'98. Conference Proceedings (Cat. No.98CH36259), Nice, France (1998)
13. N. Burlet, Platform Motion Estimation of a Low Frequency Synthetic Aperture Sonar for Buried Objects Detection, SeaTechWeek, Brest, France (2010).
14. D. Billon, What limits the resolution of the synthetic aperture sonars?. Proc. International Conference on Acoustics. (2004). p. 1921-1924.
15. S. Delayes, N. Burlet, Y. Le Gall, J.P. Malkasse, SAMDIS a multi view SAS, UDT (2022)
16. S. Leier, J. Groen, A. M. Zoubir, U. Hölscher, I. Campbell, The Influence of Sound Speed on Synthetic Aperture Sonar Imagery, UACE (2013)
17. M. Chabah, N. Burlet, J.P. Malkasse, G. Bihan, B. Quéllec, SAMDIS: A New SAS Imaging System for AUV, MOQESM14 and in book: Quantitative Monitoring of the Underwater Environment pp.107-118, (2016)
18. J.P. Malkasse, S. Dugelay, N. Burlet, Y. Le Gall, M. Simon, Multiple Views In Single Path Synthetic Aperture Sonar For Mine Counter-Measures Classification And Pre-Identification, submitted to Electronics Letters, Institution of Engineering and Technology, special issue on Recent Advances in Synthetic Aperture Sonar Technology (2023)
19. D. A. Cook, D. C. Brown, Synthetic Aperture Sonar Image Contrast Prediction, in IEEE Journal of Oceanic Engineering, vol. 43, no. 2, pp. 523-535 (2018)
20. F. Florin, I. Quidu, N. Le Bouffant, Naig, Shadow classification performances evaluation of Mine Hunting Sonar, Proceedings of Undersea Defence Technology, Singapore (2003)
21. E. Renne, S. Delayes, MCM program evaluation and evolutions, Combined Naval Event (2023)